J. At. Mol. Sci.
doi: 10.4208/jams.021516.042216a

Vol. 7, No. 2, pp. 64-76
May 2016

External electric field dependent photoinduced charge transfer in Donor-PC71BM system for an organic solar cell

Xiaoling Fu[a], Qiao Zhou[a], Yong Ding[a,b], Peng Song[a,b,c,*] and Fengcai Ma[a,b,*]

[a] *Department of Physics, Liaoning University, Shenyang, China*
[b] *Liaoning Key Laboratory of Semiconductor Light Emitting and Photocatalytic Materials, Liaoning University, Shenyang 110036, P. R. China*
[c] *State Key Laboratory of Molecular Reaction Dynamics, Dalian, China. Institution of Chemical Physics, Chinese Academy of Sciences, Dalian, China*

Received 15 February 2016; Accepted (in revised version) 22 April 2016
Published Online 25 May 2016

Abstract. We use time-dependent density functional theory together with a set of extensive multidimensional visualization techniques to characterize the field-dependent electronic structure and rate of photo-induced charge transfer in organic donor -acceptor dyad. External electric field is incorporated into the generalized Mulliken-Hush model and Marcus theory. We use these methods to evaluate the influence of the external electric field on the electronic coupling between donor and acceptor. We also calculate the reorganization energy and the free energy change of the electron transfer. These theoretical methods and calculation techniques proves that the external electric field has main effect on the electron transfer rate. More important, our results provide a new framework to understand charge transfer of organic systems under the external electric field.

PACS: 31.25.Jf, 82.39.Jn

Key words: external electric fields; light-induced charge transfer; electronic coupling; organic solar cell.

1 Introduction

Solution-processed bulk-hetero-junction photovoltaic cells were first reported in 1995 [1-2]. It took another 3-4 years until the scientific community realized the huge potential of

*Corresponding author. *Email addresses:* songpeng@lnu.edu.cn (P. Song), fcma@lnu.edu.cn (F. C. Ma)

this technology. And suddenly in 1999, the number of publications in that field started to rise exponentially [3]. Since then, organic materials are becoming more and more attractive due to their numerous advantages for cite an instance low cost, flexibility, large-area capability and easy processing [4]. They play an important role in fabricating of transistor, photodiodes, solar cells, and so on. From what has been discussed above and the current understanding, the photon-to-charge conversion in organic photovoltaic (OPV) devices can be described as a sequence of basic steps [1]. Therefore, charge transfer is the main aspect of the power conversion efficiency of OPV device.

In order to promote deeper understanding of the charge transfer, we pay more attention to investigate the dissociation of the photo-generated excitons into separate charges. The electron transfer rate can be estimated by Marcus theory as shown in following equation:

$$k=\sqrt{\frac{4\pi^3}{h^2\lambda k_\beta T}}|V_{da}|^2\exp\left[-\frac{(\Delta G+\lambda)^2}{4\lambda k_\beta T}\right] \tag{1}$$

where λ represents the reorganization energy, V_{DA} is the electronic coupling (charge-transfer integral) between donor and acceptor, ΔG is the Gibbs free energy change for the electron transfer reaction, kB is the Boltzmann constant, h is the Planck constant, and T is the temperature, which is set as 300K in our calculations. PCE is dominated intricately by many factors on the mentioned electron processing, the effective coupling of donor and acceptor V_{DA} is a key parameter. Several years ago, Cave and Newton introduced the generalized Mulliken-Hush (GMH) method. The GMH method has been employed for estimating electronic coupling in various systems [5].

Among all kinds of OPVs, bulk heterojuction (BHJ) OPV is one of the best OPV device architectures so far, which composed of a blend of donor (D) and acceptor (A) components [6]. And in these paper, we chose a system with [6,6]-phenyl-C71-butyric acid methyl ester ($PC_{71}BM$) as acceptor material to obtain higher PCE. As for the donor, we had a strict comparison before deciding. We designed a series of D-A copolymers using BTI as acceptor unit with different donor units. Finally, we believe that cyanomethylene-CPDT-BT will be a promising candidate for superior performance BHJ OPVs using PC71-BM as an acceptor material [6].

There are three elementary electronic processes photo-excitation. Firstly, active layer absorbs the solar photons to create electron-hole pairs; besides it will dissociating into free holes and electrons in the D/A interface; thirdly holes and electrons mobile through the donor and acceptor channels to anodes and cathodes respectively; then the charges will be collected by the electrodes [7]. Base on above, we found that electron-hole pairs play an important role in these processes. While, there is no answer to the specific impact of external electric field on electron-hole pairs. In this paper, we will discuss how the external electric field enables efficient long-range charge separation and the electron transfer rate in organic bulk heterojunction. The paper is organized as follows: Section 2 displays the theoretical methods used for the calculation external electric field dependent rate of electron transfer. We will consider the external electric field on the basis of

Marcus theory. Then Section 3 shows (i) Excited state properties. (ii) Charge transfer integral. (iii) Reorganization energy. (iv) Free energy change. In the last, the conclusions are summarized in Section 4.

2 Theoretical methods

2.1 Model

Making a bulk heterojunction (BHJ) of the conjugated polymer (the electron donor) and the electron acceptor is a good way to improve the solar cell performances. Because interpenetrating network of the BHJ increases the interfacial area between the donor and acceptor, resulting in improved solar cell efficiency [8]. Along with the ultrafast photoinduced electron transfer between the conjugated polymer and fullerene then fullerenes are widely used as an acceptor than a second polymer or a small molecule so far.

Base on the above, in a polymer fullerene solar cell, the most commonly used fullerene derivative is phenyl-C71-butyric acid methyl ester (PC71BM) [6]. As for the donor, we had a strict comparison before deciding as follow. A D-A copolymer PDTSBT, which is composed of dithienosilole (DTS) donor moiety and benzothiadiazole (BT) acceptor moiety, exhibiting broad absorption spectrum and good hole transport property. Simultaneously, the PCE of OPV device constructed from PDTSBT/PC71BM reached 5.1% [9]. Subsequently, Marks and colleagues synthesized a improved D-A copolymer PDTSBTI(1) with bithiopheneimide (BTI) unit and the OPV constructed from PDTSBTI(1)-PC71BM showed a high PCE of 6.41% [10]. Then, Shuang-Bao Li and coworkers combined the advantages of BTI, and designed a series of D-A copolymers 2-5 using BTI as acceptor unit with different donor units cyclopentadithiophene-CPDT(2), methylene-CPDT (3), cyanomethylene-CPDT(4), and biscyanomethylene-CPDT(5), respectively. The results compare with system PDTSBTI(1) showed that the device based on cyanomethylene-CPDTI-PC71BM heterojunctions has fast kintez-CT and slow kinter-CR which will further improve the PCE. Therefore, it is reported that cyanomethylene-CPDT(CC) will be a promising candidate for superior performance BHJ OPVs using PC71BM(P) as an acceptor material [6].

And on this basis, we chose PDTSBTI-PC71BM as the donor with the acceptor PC71BM. The molecular structures of system 4 and PC71BM can be seen in Fig. 1.

2.2 Parameters in Marcus expression

In organic solar cells, the PCE is dominated intricately by many factors on the mentioned electron processing, which are mainly classified into three dominant ones, namely, electronic coupling VDA, ΔG and reorganization energy λ. Pay attention to the change of these aspect under different external electric field is the main way to consider the charge separation takes place under the influence of an external electric field.

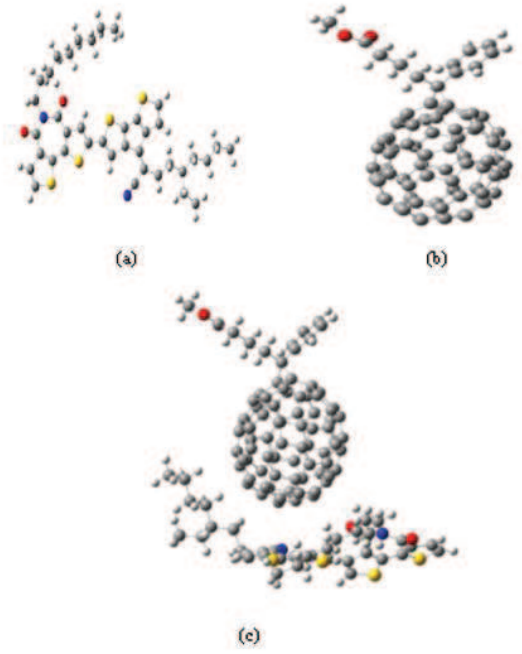

Figure 1: Molecular structures of cyanomethylene-CPDT-BTI(a), PC71BM (b), and model of the cyanomethylene-CPDTI-PC71BM complex (c).

Based on the Generalized Mulliken-Hush (GMH) formalism, the electronic coupling can be computed and the expresses is given in the following equation [11]:

$$V_{DA} = \frac{\mu_{tr}\Delta E}{\sqrt{(\Delta\mu)^2+4(\mu_{tr})^2}} \tag{2}$$

here ΔE is the vertical excitation energy, μtr is the transition dipole moment along the donor to acceptor, $\Delta\mu$ is the difference of permanent dipole moment between the initial and final states. Which was calculated using the Hellmanne Feynman theorem, as the analytical derivative of the excited-state energy with respect to an applied electric field [7].

The transition energy dependent on the static electric field Fext can be expressed as:

$$E_{exc}(F) = E_{exc}(0) - \Delta\mu F - \frac{1}{2}\Delta\alpha F^2 \tag{3}$$

where $E_{exc(0)}$=ΔE is the excitation energy at zero field, $\Delta\alpha$ is the charge in the polarizability.

For the exciton dissociation and charge recombination, ΔG is marked as ΔG_{CT} and ΔG_{CR}, respectively. The ΔG_{CR} can be rewritten as

$$\Delta G_{CR} = E_{IP}(D) - E_{EA}(A) \tag{4}$$

where EIP(D) is the ionization potential of the donor and EEA(A) is the electron affinity of the acceptor. These quantities are normally estimated from the energies of the highest occupied molecular orbital and lowest unoccupied molecular orbital of the donor and acceptor, respectively [12].

The ΔG_{CT} can be evaluated by following equation [13-14]:

$$\Delta G_{CT} = -\Delta G_{CR} - \Delta E_{0-0} - E_b \tag{5}$$

where ΔE_{0-0} is the energy of the lowest excited state of free-base donor and E_b is the exciton binding energy. And the external electric field dependent Gibbs free energy change can be written as:

$$\Delta G_{fext} = \Delta G(0) - \Delta \mu F_{ext} \tag{6}$$

Then according to the Eq. (6), we can calculated the exciton dissociation and charge recombination under the different external electric field.

Furthermore, the total reorganization energy (λ) is consists of internal reorganization energy (λ_{int}) and external reorganization energy (λ_{ext}). The inner reorganization energy arises from the change in equilibrium geometry of the donor and acceptor sites consecutive to the gain or loss of electronic charge upon electron transfer. The outer reorganization energy is due to the electronic and nuclear polarization relaxation of the surrounding medium. The inner reorganization energy upon electron transfer consists of two terms:

$$\lambda = \lambda_1(A) + \lambda_2(D) \tag{7}$$

$$\lambda_1(A) = E(A^-) - E(A) \tag{8}$$

$$\lambda_2(D) = E(D) - E(D^+) \tag{9}$$

where, $E(A^-)$ is the energies of the neutral acceptor at the anionic geometry and $E(A)$ is the energies of the optimal ground state geometry, and $E(D)$ and $E(D^+)$ express the energies of the radical cation at the neutral geometry and optimal cation geometry, respectively.

2.3 Quantum chemical calculations

In the present work, density functional theory (DFT) and time-dependent DFT (TD-DFT) are employed to calculate the geometric structure, electronic properties and optical absorption of all polymers. Based on the model we chosen , the ground-state geometries of system PDTSBTI-PC71BM was optimized by B3LYP/6-31G(d) method, which has been demonstrated to present a reasonable description of the heterojunction structure by Troisi and co-workers [15] and the initial structures are shown in Fig. 1. As for the excited-state energy, calculated at the CAM-B3LYP/6-31G(d) level. The long-range-corrected CAM-B3LYP functional was proved to be more appropriate for inter-CT excitations between D and A. And the oscillator intensities within the framework of TD-DFT was calculated at the CAM-B3LYP/6-31G(d) level [6]. Absorption spectra and CDD maps of heterojunctions were simulated by Gausssum 2.2. All the above model calculations were performed in the Gaussian 09 software package.

3 Results and discussion

3.1 Excited state properties

Selected electronic transition energies and the corresponding oscillator strengths, main compositions and CI coefficients of CCP dyad are all the main way of electron transfer

Table 1: Selected electronic transition energies (eV) and the corresponding oscillator strengths (f), main compositions and CI coefficients of CCP dyad.

states	transition energy(ev)	f	CI
S1	2.0166 (614.83 nm)	0.0013	0.49518(H→L+1)
S2	2.0928 (592.42 nm)	0.0095	0.50991(H→L)
S3	2.1490 (576.93 nm)	0.0204	0.37734(H→L+1)
S4	2.4141 (513.58 nm)	0.0198	0.59433(H-1→L+1)
S5	2.4352 (509.14 nm)	0.0294	0.54585(H→L)
S6	2.5274 (490.56 nm)	0.0206	0.45629(H-1→L+2)
S7	2.5702 (482.40 nm)	0.0042	0.42651(H-2→L)
S8	2.6217 (472.92 nm)	0.0392	0.41285(H-2→L+2)
S9	2.6478 (468.26 nm)	0.0046	0.52715(H-3→L+1)
S10	2.6863 (461.53 nm)	0.0320	0.39893(H-2→L)
S11	2.7108 (457.38 nm)	0.0137	0.32660(H-5→L)
S12	2.7298 (454.19 nm)	0.0343	0.34406(H-3→L)
S13	2.7579 (449.57 nm)	0.0091	0.45763(H-3→L+2)
S14	2.8312 (437.93 nm)	0.0835	0.25578(H→L+3)
S15	2.8460 (435.65 nm)	0.0448	0.33639(H-4→L+1)
S16	2.9377 (422.05 nm)	0.0251	0.36802(H-4→L+2)
S17	2.9716 (417.24 nm)	0.0087	0.46500(H-5→L+1)
S18	3.0123 (411.59 nm)	0.0170	0.42681(H-7→L)
S19	3.0357 (408.42 nm)	0.0024	0.37144(H-8→L+1)
S20	3.0466 (406.96 nm)	0.0059	0.32054(H-5→L+2)
S21	3.0729 (403.47 nm)	0.0053	0.33275(H-6→L)
S22	3.1051 (399.29 nm)	0.0159	0.25504(H-5→L+2)
S23	3.1464 (394.05 nm)	0.0249	0.30216(H→L+4)
S24	3.1847 (389.31 nm)	0.0148	0.32895(H-2→L+3)
S25	3.2141 (385.75 nm)	0.0125	0.32895(H-5→L+2)
S26	3.2671(379.49 nm)	0.0291	0.29455(H-3→L+3)
S27	3.2895 (376.91 nm)	0.0149	0.39084(H-7→L+1)
S28	3.3136 (374.17 nm)	0.0110	0.43433(H-8→L)
S29	3.3206 (373.37 nm)	0.0317	0.24718(H-2→L+3)
S30	3.3303 (372.29 nm)	0.0728	0.36220(H-1→L+3)
S31	3.3718 (367.71 nm)	0.0005	0.30129(H-9→L)
S32	3.4352 (360.92 nm)	0.0477	0.25068(H-10→L)
S33	3.4447 (359.92 nm)	0.0858	0.33554(H→L+5)
S34	3.4643(357.90 nm)	0.0159	0.44829(H-5→L+3)
S35	3.4807 (356.21 nm)	0.0107	0.26059(H-10→L)

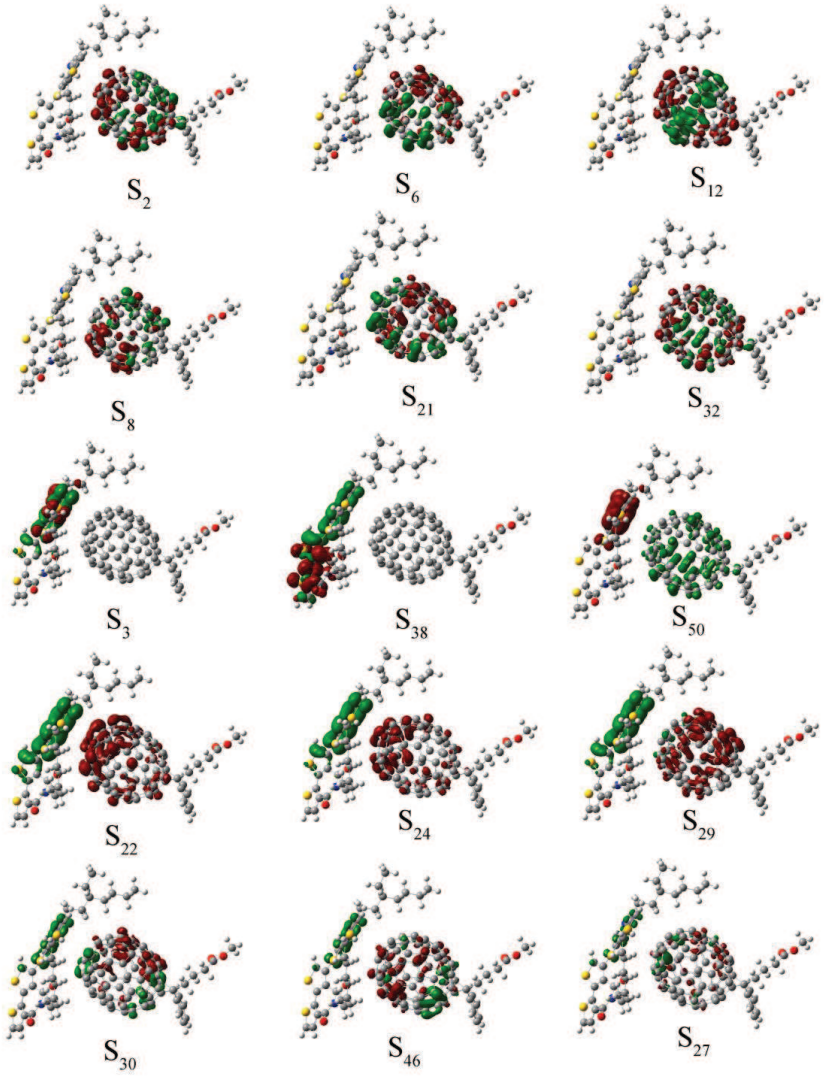

Figure 2: Selected CDDs of CCP dyads with 3×10-5 au external electric field. (Green and red color represents the hole and electron, respectively).

rate, and we start research them without external electric fields. They all belong to the excited state properties. The calculation is summarized in Table 1. To directly observe the charge transfer process, we plotted the CDD maps, which show the electron-hole coherence of the charge transfer is visualized in Fig. 2 and Fig. 3. And it is clear to see the electron density is increased or decreased during the charge transition process from Fig. 2 and Fig. 3. We notable that the charge transfer is affect by the external electric field. Following which, we consider the effects of the external electric field on the charge transition process focusing on the three ways: transition energy, transition

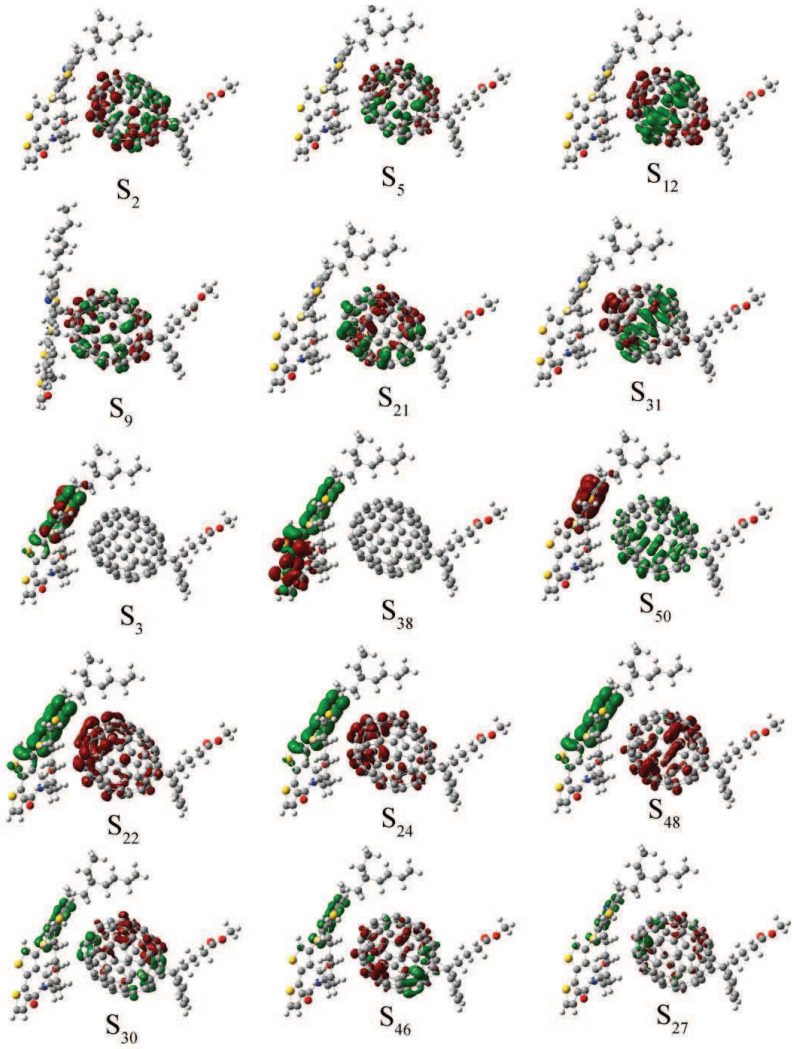

Figure 3: Selected CDDs of CCP dyads with -20×10-5 au external electric fields. (Green and red color represents the hole and electron, respectively).

dipole moment, and other excited-state properties of the CPM dyad. All parameters were calculated by using the TDDFT method.

3.2 Charge transfer integral

For organic solar cells, the transport of the charges occurs under the influence of an external electric field. Therefore, we will now study properties of excited states under the external electric field. The influence of the external electric field on the VDA reflected in Eq. 2. The relationship between $\Delta\mu$ and $\mu_{ij}(F_{ext})$ at different strength of F_{ext} plays a key role here. From Eq. 3, we can obtain $\Delta\mu$. And consider the direct quantum chemical

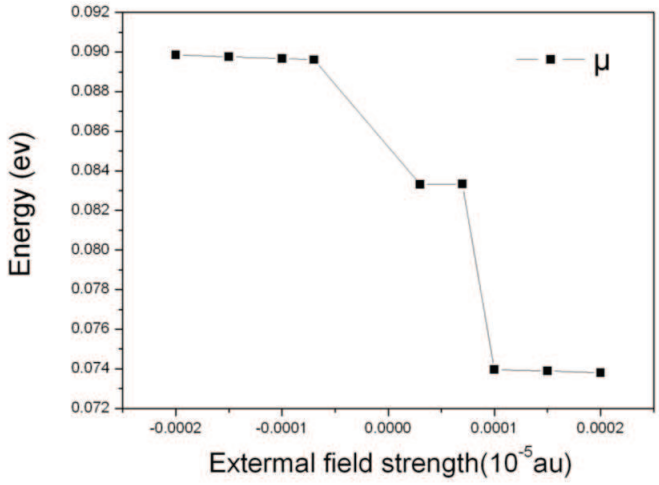

Figure 4: The difference of permanent dipole moment between the initial and final states calculated by using Eq. 3.

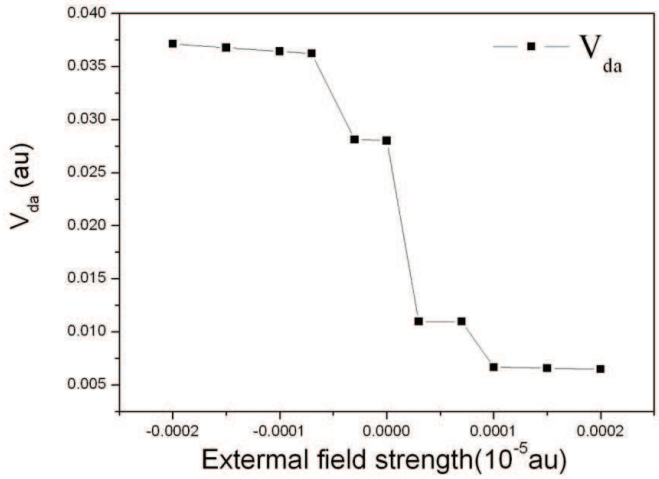

Figure 5: Electronic coupling VDA calculated by using Eq. 2.

calculations of $\mu_{ij}(F_{ext})$ for selected excited-states of cyanomethylene-CPDTI-PC_{71}BM are plotted as a function of the amplitude of the external electric field in Fig. 4.

Since the S_5 excited-state of cyanomethylene-CPDTI-PC_{71}BM complex is localized excited state, $V_{DA}(S_0 \rightarrow S_5)$ was estimated and is characterized as the lowest intermolecular charge transfer excited state. The calculated μ_{tr}=0.7251 au for S_5 and the fitted $V_{DA}(S_0 \rightarrow S_5) \sim$ 0.037141. The influence of the external electric field on the V_{DA} was calculated by using Eq. 2. The calculated V_{DA} are plotted as a function of the external electric field in Fig. 5. And from the Fig. 5, we can see that the coupling strength between

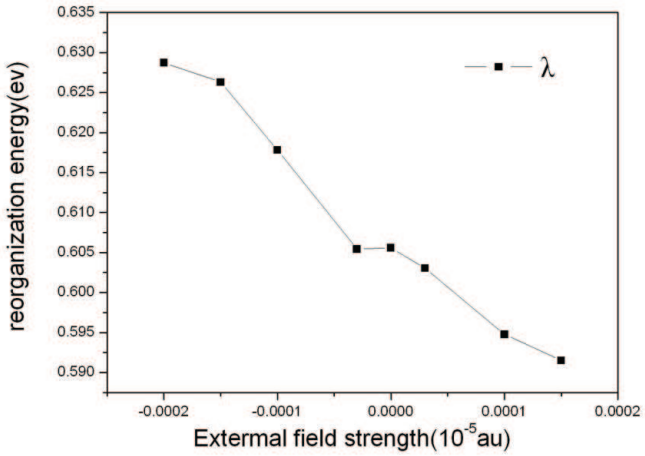

Figure 6: Reorganization energy plotted versus the external electric field.

donor and acceptor increases substantially following the increasing of external electric field.

3.3 Reorganization energy

The reorganization energy λ consists of inner reorganization energy and outer reorganization energy. The inner reorganization energy upon electron transfer consists of two terms, it could be approximately evaluated by Eq. 7. The inner reorganization energy arises from the change in equilibrium geometry of the donor and acceptor sites consecutive to the gain or loss of electronic charge upon electron transfer [16]. In general, it is mainly due to the $D^* \rightarrow D^+$ transition. As a result we obtain λ=0.3055 eV at F_{ext}=0.

For the outer reorganization energy, it is due to the electronic and nuclear polarization relaxation of the surrounding medium. But λ_{ext} is not easily estimated quantitatively in solid state. It is usually much smaller in the solids than that in liquids, but it still accounts for a good fraction of the λ. The previous experimental result illustrate that a setting λ_{ext} within the physically plausible range would modify the rate only by one order of magnitude, which is not considered to be a very large error in that context [6]. As a consequence λ_{ext} is set as 0.11 eV, which is similar to the very small reorganization energy in the photosynthetic reaction center ($\sim$0.2 eV). On the basis of these results we choose a similar value 0.3 eV, which is similar to the inner reorganization energy, was used as a constant value for λ_{ext} in our calculations. And the calculated total reorganization energies are plotted as a function of the external electric field in Fig. 6.

3.4 Free energy change

In the exciton dissociation and charge recombination, $\Delta G = \Delta G_{CT}$ and ΔG_{CR}, respectively. They are calculated using Eq. 4 and 5. The ΔG_{CR} is mainly due to the highest occupied

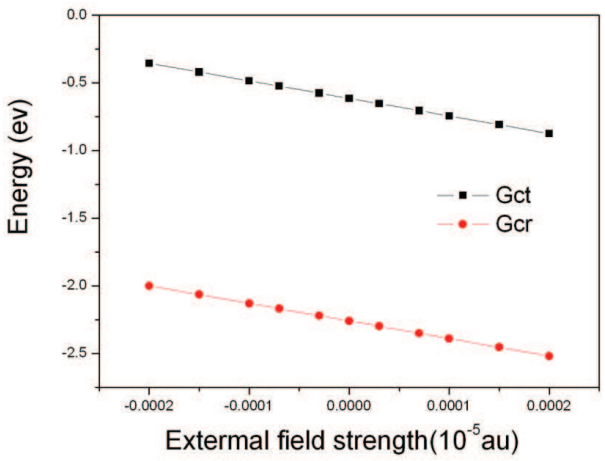

Figure 7: Gibbs free energy of the exciton dissociation and charge recombination reaction (ΔG_{CT} and ΔG_{CR}) plotted versus the external electric field.

molecular orbital (HOMO) of donor molecule and the lowest unoccupied molecular orbital (LUMO) of acceptor molecule, It is associated with the optimization of the structure of the ground-state donor and acceptor. At the same time, ΔG_{CT} is calculated on the basis of ΔG_{CR} clearly manifested in the Eq. 5. Then according to the Eq. 6, we can calculated the exciton dissociation and charge recombination under the different external electric field. And the effect of external electric field to exciton dissociation and charge recombination is reported in Fig. 7. We found that $\Delta G_{CT}(F_{ext})$ is increasingly negative with the increase of the external electric field. It is -0.354 eV when the external electric field is -20×10^{-5} au and it is -0.874 eV when the external electric field is 20×10^{-5} au. This reflects the electrostatic interaction between the separated charges and the electric field. As for the $\Delta G_{CR}(F_{ext})$, it is -2.000 eV when the external electric field is -20×10^{-5} au and it is -2.519 eV when the external electric field is 20×10^{-5} au, and it is smaller than ΔG_{CT}. That is to say compared with charge recombination, exciton dissociation is much easier.

3.5 The rate of external electric field dependent photoinduced charge transfer

We are now in a position to consider the influence of charge separation rate under the influence of an external electric field by inserting all the calculated parameters into Eq. 1, which are mainly classified into three dominant ones, namely, electronic coupling V_{DA}, ΔG and reorganization energy λ .We plot in Fig. 8 the charge separation rate. It is can be seen that the charge separation rate gets faster during the strength of the external electric field from -$20\times10^{-5} \rightarrow 0\times10^{-5}$ au and the changes of charge separation rate is not significant in ranging from $0\times10^{-5} \rightarrow 20\times10^{-5}$ au, due to the changes of ΔG ,V_{DA} and λ. At the same time, we found that the rate of charge recombination is significantly smaller than the corresponding rate of charge separation. That is also to say charge separation

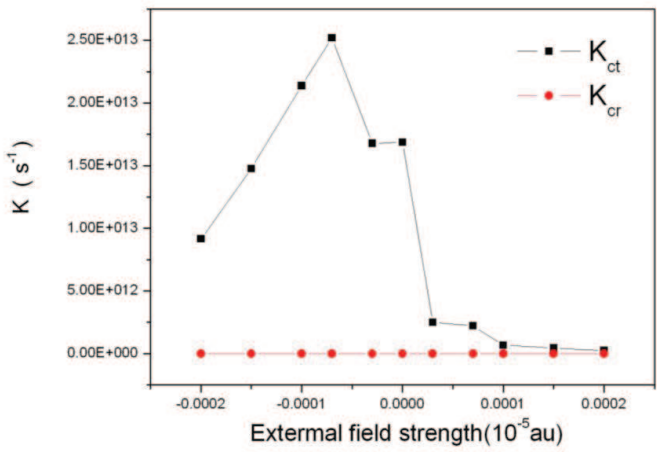

Figure 8: Calculated rate of exciton dissociation and charge recombination of CCP dyad at different external electric field.

rate is faster than charge recombination rate. This conclusion proves that the external electric field has main effect on the electron transfer rate. More important, our results provide a new framework to understand charge transfer of organic systems under the external electric field.

4 Conclusion

We use time-dependent density functional theory to characterize the field-dependent electronic structure and rate of photoinduced charge transfer in organic donor-acceptor dyad .We thoroughly analyze external field dependent charge transfer integral (V_{DA}), reorganization energy (λ), free energy (ΔG), and the rate of charge transfer (k_{CT}) with the influence of the external electric field. Finally, we found that the external electric field mainly has effect on the charge transfer integral, reorganization energy and free energy change. That is to say the external electric field has effect on characterize the field-dependent electronic structure and rate of photoinduced charge transfer in organic donor-acceptor dyad.

Acknowledgments. This work was financially supported by the National Natural Science Foundation of China (Grant Nos. 11304135 and 11544015), and the Shenyang Natural Science Foundation of China (F15-199-1-04), Liaoning Provincial Department of Education Project (Grant No. L2015200), the Program for Liaoning Excellent Talents in University, China (LJQ2014001).

References

[1] P. Song, Y. Z. Li, F. C. Ma, T. Pullerits and M. T. Sun, J. Chem. Phys. 117 (2013) 15879.

[2] C. Yu, J. Gao, J. C. Hummelen, F. Wudl, A. J. Heeger, Science 270 (1995) 1789.
[3] D. Gilles, M. C. Scharber and C. J. Brabec, Adv. Mater. 21 (2009) 1323.
[4] T. M. Clarke and J. R. Durrant, Chem. Rev. 110 (2010) 6736.
[5] A. A. Voityuka, J. Chem. Phys. 124 (2006) 64505.
[6] S. B. Li, Y. A. Duan, Y. Geng, H. B. Li, J. Z. Zhang, H. L. Xu, M. Zhang, Z. M. Su, PCCP 16 (2014) 25799.
[7] Y. Z. Li, D. W. Qi, P. Song and F. C. Ma, Mater. 8 (2014) 42.
[8] S. K. Pal, T. Kesti, M. Maiti, F. L. Zhang, JACS 132 (2010) 12440.
[9] J. Hou, H. Y. Chen, S. Zhang, G. Li and Y. Yang, JACS 130 (2008) 16144.
[10] X. Guo, N. Zhou, S. J. Lou, J. W. Hennek, R. P. Ortiz, M. R. Butler, P. L. T. Boudreault, J. Strzalka, P. O. Morin, M. Leclerc, J. T. L. Navarrete, M. A. Ratner, L. X. Chen, R. P. H. Chang, A. Facchetti and T. J. Marks, JACS 134 (2012) 18427.
[11] X. R. Liu, W. Shen, R. X. He and Y. F. Luo, J. Phys. Chem. C 118 (2014) 17266.
[12] X. Zhang, L. Chi, S. Ji, Y. Wu, P. Song, K. Han, H. Guo, T. D.James, J. Zhao, JACS 131 (2009) 17452.
[13] X. Zhang, L. Chi, S. Ji, Y. Wu, P. Song, K. Han, H. Guo, T. D.James, J. Zhao, Chem. Rev. 86 (1986) 401.
[14] G. J. Kavarnos, N. J. Turro, JACS 131 (2009) 15777.
[15] T. Liu and A. Troisi, J. Phys. Chem. C 115 (2011) 2406.
[16] P. Song, Y. Z. Li, F. C. Ma, T. Pullerits and M. T. Sun, Chem. Rec. 16 (2016) 3.